

Abundance analysis of roAp stars

V. HD 166473*

M. Gelbmann¹, T. Ryabchikova^{1,2}, W.W. Weiss¹, N. Piskunov³, F. Kupka¹, and G. Mathys⁴

¹ Institute for Astronomy, University Vienna, Türkenschanzstrasse 17, 1180 Vienna, Austria (last_name@galileo.astro.univie.ac.at)

² Institute of Astronomy, Russian Academy of Sciences, Pyatnitskaya 48, 109017 Moscow, Russia (ryabchik@inasan.rssi.ru)

³ Uppsala Astronomical Observatory, Box 515, 751 20 Uppsala, Sweden (piskunov@astro.uu.se)

⁴ European Southern Observatory, Casilla 19001, Santiago 19, Chile (gmathys@eso.org)

Received 10 December 1999 / Accepted 20 January 2000

Abstract. This fifth paper in a sequence on abundance analyses of roAp stars features several improvements and complements over the previous investigations:

- i. The new VALD–2 atomic data base was used which significantly improves the analysis of C, N, O, and rare earth elements (REE) and in particular includes also some doubly ionized REE species.
- ii. An individual opacity distribution function table was generated for a successful synthesis of photometric indices of this very peculiar star.
- iii. The influence of a (rather strong) magnetic field on abundance determinations is studied and presented for 30 elements.
- iv. Our investigation of 33 elements (45 ions) is the hitherto most complete chemical analysis of a chemically peculiar star, using modern tools.

Similar to the four roAp stars analysed by us so far (α Cir: Kupka et al. 1996, HD 203932: Gelbmann et al. 1997, γ Equ: Ryabchikova et al. 1997a, and HD 24712: Ryabchikova et al. 1997b) we find nearly solar abundances of Fe and Ni, and a definite overabundance of Cr and especially Co. Rare earth elements have large overabundances, whereas C and O are underabundant relative to the Sun. This pattern seems to be a common property of the chemically peculiar (CP2, Ap) stars.

A new and most striking result is the discovery of the anomalous line strengths of the second ions of REE resulting in an abundance increase of up to +1.5 dex, compared to values obtained from lines of the first ions. This anomaly is not found in non-roAp and “normal” stars.

Key words: stars: abundances – stars: atmospheres – stars: chemically peculiar – stars: fundamental parameters – stars: individual: HD166473

1. Introduction

Rapidly oscillating Ap (roAp) stars are a cool subgroup of CP2 stars and oscillate usually with multiple periods ranging from a few minutes up to about 20 minutes. Considering their position on the HR-diagram which implies a mass between one and two solar masses, such short periods are indicative for non-radial, high overtone, low order acoustic p -modes. According to the hitherto most successful oblique pulsator model (Kurtz 1982) pulsation and magnetic field axes are aligned, but oblique to the axis of rotation. This scenario and other characteristics of roAp stars are well described in various reviews (e.g., Kurtz 1990, Matthews 1997, and references therein).

The purpose of our project on abundance analyses of roAp stars is to provide accurate fundamental parameters of this astrophysically very interesting group of stars which constitutes an unique laboratory for testing important domains of stellar pulsation theory and of magneto-hydrodynamics communicated through oscillation (Gautschy et al. 1999, Matthews et al. 1999). In particular we derive T_{eff} , $\log g$, abundances and magnetic field parameters which provide important boundary conditions needed for stellar pulsation models and we investigate the effects of a surface magnetic field on abundance determination.

The roAp star HD 166473 (CD $-37^{\circ}12303$, V694 CrA) with $V = 7.95$ mag is classified by Houk (1982) as an Ap(SRCREU) star. Hauck & Mermilliod (1980) list Strömgren indices of $b - y = 0.213$, $m_1 = 0.311$ and $c_1 = 0.538$. Based on $\beta = 2.801$ (Martinez 1993), and using Crawford’s (1979) A-type star calibration we determine $\Delta m_1 = -0.127$ and $\Delta c_1 = -0.101$. Both indices are the most negative of all known roAp stars, except for Przybylski’s star. The dominating pulsation frequency is at 1.892 mHz with a peak-to-peak amplitude of 0.49 mmag (Kurtz & Martinez 1987).

A variable surface magnetic field ranging from 8.6 to 6.4 kG was discovered by Mathys et al. (1997) using high-resolution spectra in the region centered on λ 6150 Å. The average of these spectra was used for our abundance analysis. The variation of the magnetic field modulus indicates a very long period beyond 3 yr which implies a $v \cdot \sin i$ of clearly less than 1 km s⁻¹. Both effects, slow rotation and large magnetic field,

Send offprint requests to: Werner W. Weiss

* Based on observations obtained at the European Southern Observatory (La Silla, Chile)

are responsible for intensification effects in specific spectral regions which strongly depend on the atomic line Zeeman pattern, and which cannot be described any more in terms of magnetic “pseudo-microturbulence”, a successful concept, e.g., for γ Equ (Ryabchikova et al. 1997a) and HD 24712 (Ryabchikova et al. 1997b). In the following we present the results of our abundance analysis for HD 166473 based on synthetic spectra which include magnetic field effects in the radiation transfer.

2. Observations

The ESO-NTT set-up as described in Gelbmann et al. (1997) was used for the observations and all subsequent reductions, merging of echelle orders to one continuous spectrum and normalization to the continuum were done with IRAF and are referred to as “low resolution spectra” in this paper. The Abundance Analysis Procedure software package AAP (Gelbmann 1995) was used to derive the basic stellar parameters and abundance pattern. If not mentioned otherwise, all procedures were the same as described in our series of Paper I to Paper IV.

An additional high resolution spectrum (ESO CAT-CES instrument, $R=122000$) ranging from 6123 to 6178 Å which shows resolved Zeeman components was available. This spectrum is an average of six individual spectra which were observed almost at the same phase and close to magnetic maximum and they are described in Mathys et al. (1997).

3. Model atmosphere

To determine atmospheric parameters and abundances for a star with peculiarities similar to HD 166473 is quite difficult. In Sect. 1 it was already mentioned that this star has the most peculiar photometric colours next to Przybylski’s star (HD 101065) which probably are a result of a large overabundance of rare earth elements (see Sect. 4.3). Only HD 101065 appears to be even more abnormal in this respect.

To determine the starting values for the model atmosphere of HD 166473 we used the software package TEMPLOGG (Rogers 1995) which takes advantage of calibrations of the Strömgren system (Crawford 1979, and subsequent calibrations) and we derived a $T_{\text{eff}} = 7900$ K and $\log g = 4.4$. For the initial model atmosphere we used $[M/H] = +1.00$, which is close enough to the photometric estimate of $[M/H] = +1.27$ and which is a standard abundance value for Kurucz’s scaled solar model atmospheres (Kurucz 1993). For the microturbulent velocity an artificially high value of $v_{\text{micro}} = 4.0$ km s⁻¹ was chosen, simply to compensate for missing magnetic intensification caused by a field of 8.6 kG. The naming convention used for the models includes T_{eff} , $\log g$, $[M/H]$, and v_{micro} , for example: 7900g44p10k4.

The final synthetic spectrum was computed with the SYNTHMAG code (Piskunov 1999), based on a radiation transfer in the presence of a magnetic field. The large microturbulence was used only for model calculations, while for spectrum synthesis the microturbulence was set to zero, because a strong magnetic field suppresses any turbulent motions, which is corroborated by the investigation of other roAp stars (see Paper I – Paper IV).

After several iterations of the whole synthesis procedure (for technical details see Gelbmann et al. 1997, Gelbmann 1998), we arrived at a compromise model with the following parameters: $T_{\text{eff}} = 7700$ K, $\log g = 4.2$, and $[M/H] = +0.50$. Unfortunately, this model does not satisfy all criteria for a consistent spectrum analysis. Although it reproduces reasonably well the H β line, the Strömgren colours, and provides an ionization equilibrium, it still cannot remove a slight dependency of the abundance on the lower levels excitation energy of spectral lines for both Fe I and Fe II. A higher temperature would be needed to remove this trend, but simultaneously it would degrade the fit to photometric indices and the H β line profile. On the other hand, a Kurucz model atmosphere with $v_{\text{micro}} = 2$ km s⁻¹, $T_{\text{eff}} = 7250$ K, $\log g = 4.5$, and $[M/H] = +1.00$ formally reproduces well the Strömgren indices, but does not fit any more the H β line profile. The value for $\log g = 4.2$, determined spectroscopically with the procedure previously described and using a higher microturbulence, is more appropriate for a main sequence star and hence was chosen for the “final” model atmosphere.

Another serious shortcoming of the traditional approach comes from the peculiar chemical composition of the atmosphere. The deviation of the abundance pattern of HD 166473 from the solar values affects the $[M/H]$ determination, which is calibrated for main sequence stars with scaled solar abundances. Particularly, the rare earth elements (REE) are important, because they have spectra with more spectral lines than the iron peak elements and hence contribute much to the line opacities. Unfortunately, our knowledge of the atomic parameters of REE is limited to a few thousand lines of the neutral and first ionized species, while we include millions of iron peak element lines. Moreover, the total number of REEs exceeds the total number of iron peak elements.

The following experiment illustrates the importance of the specific chemical abundance in model atmosphere calculations. On average, REE are overabundant in HD 166473 by +2.8 dex. We calculated opacity distribution functions (ODFs) for Przybylski’s star which is extremely overabundant in REE by about +4.0 dex and deficient in CNO. In order to compensate for the missing line opacities due to insufficiently known REE spectral lines we increased the overabundance of the iron peak elements to +1.5 dex. All calculations were performed with the procedure developed by Kupka & Piskunov (Kupka & Piskunov 1998; Piskunov & Kupka 2000).

Table 1 compares the observed Strömgren indices of HD 166473 with three sets of synthetic indices. The first set is produced from a scaled solar abundance Kurucz’ model with $T_{\text{eff}} = 7700$ K, $\log g = 4.2$, $[M/H] = +0.50$, and $v_{\text{micro}} = 0$ km s⁻¹, the second differs only by a $v_{\text{micro}} = 4$ km s⁻¹. The third set is obtained with a model of $T_{\text{eff}} = 7550$ K, $\log g = 4.2$, and $v_{\text{micro}} = 1$ km s⁻¹ but with an ODF developed for Przybylski’s star which resembles the abundance pattern of HD 166473.

The results presented in Table 1 illustrate the possibility to reproduce the observed colour indices (except for m_1 in this case) even for most peculiar objects provided that the peculiar chemical composition of CP stars correctly is taken into

Table 1. Comparison of observed and calculated Strömgren indices of HD 166473 for Kurucz’s model atmospheres using scaled solar abundances (scaled) and using a more realistic, but not yet optimized opacity distribution function (ODF) table.

Index	Obs.	scaled		ODF
		$v_{\text{micro}}=0$	$v_{\text{micro}}=4$	
$b-y$	0.213	0.143	0.130	0.202
m_1	0.311	0.263	0.265	0.484
c_1	0.538	0.813	0.842	0.534
β	2.801	2.792	2.801	2.798

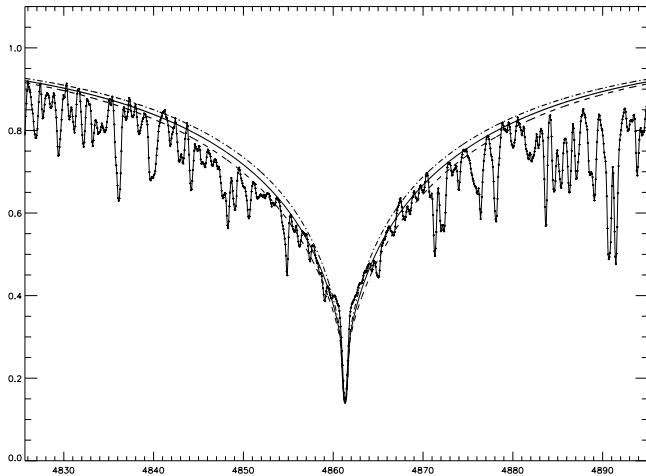


Fig. 1. Comparison between the observed $H\beta$ line profile and three different synthetic profiles. The solid line represents the model 7700g42p05k4, the dashed line – 8000g42p05k4, and the dash-dotted line – 7500g42p05k4.

account. An analysis based on the 7550g42.ODF model still cannot remove the previously mentioned trend of line abundances versus lower excitation energy levels. The ODF model, however, provides the same average Fe peak element abundance as our adopted “final” model.

For the following reasons we did not use our ODF model (adapted for Przybylski’s star) for the abundance analysis of HD 166473:

- Missing line opacities from REE were substituted by enhanced lines of the iron peak elements, but both groups of elements have a different distribution of lines over the entire spectral range.
- A direct comparison of abundances for HD 166473 with the abundances determined for other roAp stars, but which are based on scaled solar composition models, would be difficult.

The Balmer hydrogen lines are sensitive to T_{eff} . The profiles of $H\alpha$ and $H\beta$ were calculated for a set of models, compared with the observations, and a possible range of $T_{\text{eff}}=7500$ K to 8000 K was determined. Hence, the formal error in our effective temperature determination is ± 250 K. The error of the surface gravity is estimated to ± 0.2 dex. Fig. 1 shows a comparison of the observed $H\beta$ line with three different synthetic profiles.

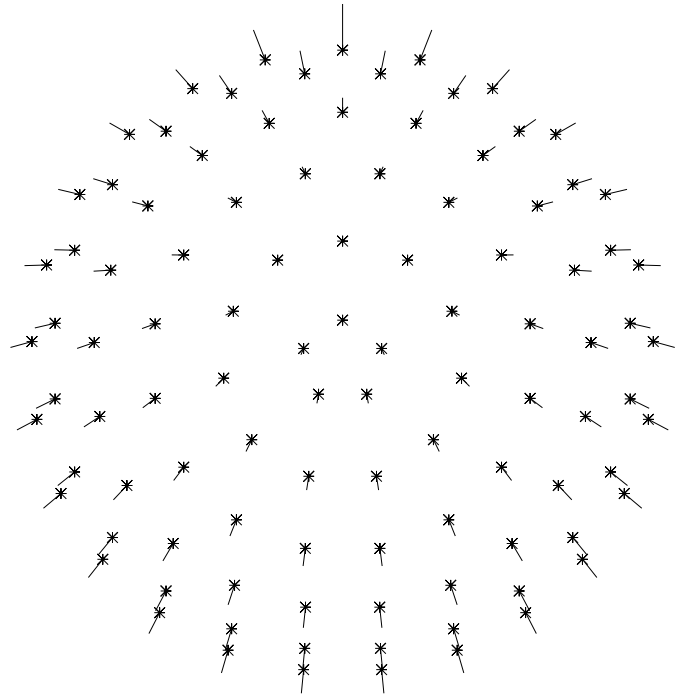


Fig. 2. Magnetic surface field vectors derived from our model which is used to compute the Stokes I component for our synthetic spectra

3.1. Magnetic field modelling

The strong magnetic field in HD 166473 has to be taken into account in an abundance analysis. Radiation transfer calculations in the presence of a magnetic field were implemented in the spectrum synthesis code (Piskunov 1999) and applied to Eu lines in magnetic CP stars (Ryabchikova et al. 1999b) as a test.

First we had to determine a magnetic field configuration which reproduces the Zeeman pattern of the lines observed in the high resolution spectrum which ranges from 6123 to 6178 Å. As observations of only a single phase are available we cannot determine a complete magnetic field model, and we have to accept that our “solution” will be far from unique. As a matter of fact, a large variety of more-or-less complicated field geometries with various multipole components allows the reproduction of the Stokes I component as is observed in our spectrum within the observational errors. We considered it reasonable for our abundance analysis to choose the magnetic model which is the simplest and has a minimum of free parameters.

To determine such a model we used the program INVERS10 (Piskunov 1999) which originally was written to solve the inversion problem and to perform magnetic Doppler imaging. We applied this code in the “direct” mode, i.e. we assumed a magnetic field geometry and computed the disk integrated spectrum. It was not possible to reproduce the high resolution spectrum with a centered dipole and even off-sets of 0.5 radii were not sufficient, hence we investigated more complex models. A de-centered dipole (polar field strength of 10 kG) with the magnetic center close to the stellar surface, the magnetic axes perpendicular to the rotation axes, and with a radial field component of +1 kG superposed (Fig. 2) produced a satisfactory fit. Such a

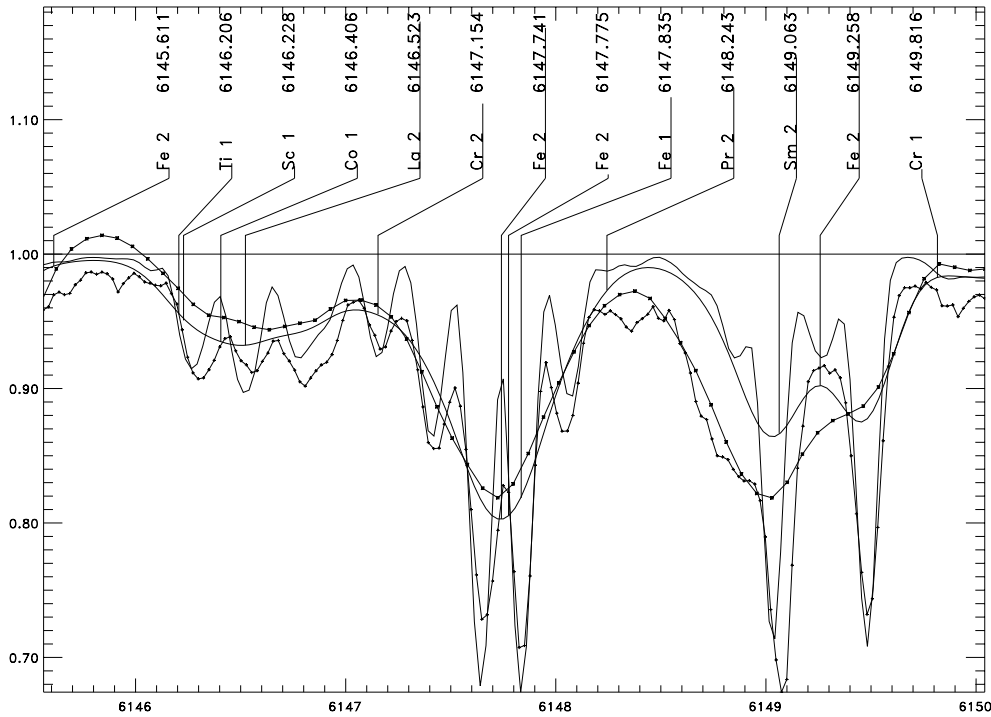


Fig. 3. Thin line with +: high resolution observations, thin line with x: low resolution spectrum, full lines: synthetic spectra convolved with the instrumental profiles for, respectively, the high and low resolution spectra. Note the line close to 6148.8 which is missing in our atomic line data base.

field geometry definitely does not represent the actual geometry for HD 166473, but on the level of a *phase snapshot disk average* it reproduces well the Stokes *I* components of our observations. A refinement of this model was considered not to be critical for the interpretation of the low resolution spectra which, however, were the basis of our abundance analysis.

The chosen 3-D model with 200 surface elements fits both observed spectra: the high resolution (instrumental broadening of 0.08 \AA) and small spectral range spectrum with clearly visible Zeeman pattern and also the spectrum with lower resolution (instrumental broadening of 0.3 \AA), but wide spectral range (Fig. 3.1). For the latter spectrum we found negligible differences between a synthesis based on a detailed 3D magnetic field model, and on a simpler model which assumes a plan-parallel atmosphere with a radial magnetic field component of 7 kG and a field component parallel to the surface of 5 kG at every surface point. As the final abundance analysis had to use a spectral range as wide as possible, the relevant issue was to model efficiently the low resolution spectrum. Hence, to save significant computing time this analysis was carried out with the program SYNTHMAG (Piskunov 1999) which uses the simplified magnetic field geometry.

3.2. Abundance analysis

Line lists for all chemical elements were generated with the current version of VALD-2 (Kupka et al. 1999, Ryabchikova et al. 1999a), and lines in the Balmer wings as well as in spectral regions crowded with telluric lines were ignored. The most recent references for the atomic data of individual species will be given in the corresponding sections. We did not analyze the spectral region below $\lambda 5000 \text{ \AA}$ because of severe blending. The opti-

mum fit of synthetic lines to the observations resulted in a total of 366 individual “line” abundances which were appropriately averaged to determine the final abundances of 33 elements.

An example for the spectral region around 6148 \AA is given in Fig. 3.1. The large diversity of Zeeman patterns which have to be taken into account is obvious. Differences of the fit to the observations for some of the lines may also be caused by an inhomogeneous surface distribution of the elements. For our synthesis we used the same magnetic field geometry for the entire spectrum and for all the elements.

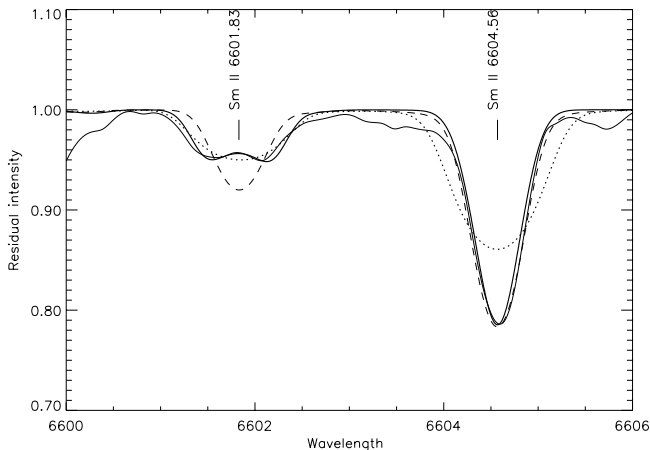
4. Element abundances

Table 2 compares the line abundances determined for unblended and only weakly blended Sm II lines for different cases. The first case corresponds to a 8.6 kG magnetic field and zero $v \cdot \sin i$ and v_{micro} model which is adopted for the final abundance analysis of HD 166473. In the two other cases we try to simulate the magnetic field broadening of lines with non-zero v_{micro} and $v \cdot \sin i$, an approach which was frequently used in the past.

It is interesting to note that with such a large field of 8.6 kG the magnetic intensification is not proportional to \bar{g}_{eff} . Lines with a relatively large \bar{g}_{eff} and a configuration close to a pseudo-triplet (e.g. $\lambda 6426.62$) split nearly completely in their components, which results in a low magnetic intensification. On the other hand, the $\lambda 6604.53$ line (see also Fig. 4) is an example for a significant magnetic broadening caused by a relatively small \bar{g}_{eff} but complex Zeeman pattern. It is obvious that the more physical model results in a clearly smaller scatter of the line abundances. This figure illustrates also a large range of *formal* $v \cdot \sin i$ values (15 to 30 km s^{-1}) needed to fit individual lines in low resolution spectra, if the magnetic field is ignored. Such an

Table 2. Line abundances for unblended and only weakly blended Sm II lines for different models of magnetic broadening. Velocities are in km s^{-1} .

λ (Å)	E_i	$\log gf$	\bar{g}_{eff}	$W_{m\text{Å}}$	line abundances		
					no magnetic field		
					$v_{\text{micro}}=0$	$v_{\text{micro}}=1$	$v_{\text{micro}}=2$
5836.32	0.998	-1.198	1.190	29.0	-8.40	-8.25	-8.36
5938.97	0.933	-1.342	0.810	15.1	-8.60	-8.57	-8.62
5963.22	1.517	-1.194	1.140	35.8	-8.00	-7.69	-7.84
6325.60	1.446	-1.195	0.750	26.0	-8.30	-8.01	-8.10
6426.62	1.746	-0.559	1.510	44.0	-8.00	-7.96	-8.18
6472.35	1.226	-1.308	1.380	28.0	-8.20	-7.99	-8.10
6601.83	1.493	-0.773	1.940	50.4	-8.25	-7.78	-8.07
6604.53	1.708	-0.237	0.680	127.3	-8.10	-6.32	-7.18
6630.61	1.517	-1.208	0.990	26.6	-8.20	-7.94	-8.04
6632.27	1.670	-0.637	1.490	51.6	-8.20	-7.75	-8.05
6687.79	1.708	-0.972	0.500	54.0	-7.90	-7.33	-7.65
6693.55	1.687	-0.373	1.500	53.8	-8.00	-7.95	-8.28
6731.81	1.166	-0.521	0.970	65.5	-8.65	-7.90	-8.36
6741.49	0.998	-0.984	1.260	91.5	-8.15	-6.87	-7.62
7139.33	1.890	-0.922	0.400	19.0	-8.30	-8.18	-8.24
7143.96	0.998	-1.063	1.500	30.9	-8.60	-8.40	-8.52
7560.04	1.687	-1.010	1.900	30.9	-8.15	-7.93	-8.05
				mean:	-8.25	-7.81	-8.07
				σ :	0.24	0.53	0.34

**Fig. 4.** Comparison of observed low resolution line profiles (thin line) for two Sm II lines at λ 6601.83 ($\bar{g}_{\text{eff}}=1.93$) and λ 6604.56 ($\bar{g}_{\text{eff}}=0.68$) with three synthetic line profiles. Thick line: synthesis for a model as is described in this paper (magnetic field, $v \cdot \sin i = 1 \text{ km s}^{-1}$ and abundances listed in Table 3); dashed line: a model without magnetic field, with $v_{\text{micro}} = 1 \text{ km s}^{-1}$, $v \cdot \sin i = 17 \text{ km s}^{-1}$, abundances of Table 3; dotted line: the same model, but with a $v \cdot \sin i = 30 \text{ km s}^{-1}$.

unrealistic situation of a variable $v \cdot \sin i$ is a direct indication for the presence of a strong magnetic field.

Table 3 summarizes the abundances of all elements investigated for HD 166473 with a model of $T_{\text{eff}} = 7700 \text{ K}$, $\log g = 4.20$, $[\text{M}/\text{H}] = 0.5$, $v \cdot \sin i = 0$, $v_{\text{micro}} = 0$, and a magnetic field of 8.6 kG. For comparison we also give the abundances obtained by a standard analysis, approximating magnetic field effects with a v_{micro} increased to 1.0 km s^{-1} and a mean $v \cdot \sin i = 18 \text{ km s}^{-1}$

(fifth column). The microturbulence was estimated from Fe lines only.

As expected, using a physically more realistic model by including effects of magnetic intensification gives lower abundances. The difference strongly depends on the adopted value of the microturbulence in the classical analysis (see Table 2). With a carefully chosen value we may decrease this difference to a minimum and come quite close to a full analysis. This is a comforting result, because within the error range of models and observations used, our previous analyses of moderate magnetic roAp stars do not have to be corrected. In some cases a nonmagnetic analysis provides even smaller abundances which may be explained with typically small Landé factors (Ce II lines) or differences in the oscillator strengths used (e.g., Dy II, Er II).

As a last comment, the abundance pattern for the heavier elements almost perfectly fits the odd-even rule (Fig. 5).

4.1. Light elements

Similar to α Cir, HD 203932 and γ Equ, the light elements C and O are underabundant. Na, Mg, Si, and S have nearly solar abundances, Al is overabundant as in γ Equ. But we observe solar Al abundance in roAp stars HD 203932 and HD 24712.

Some of the statements in the previous paragraph might have to be modified when better data become available, because they are based on only few and/or weak lines. New oscillator strength data for CNO elements were taken from the recent NIST compilation (Wiese et al. 1996).

The oxygen abundance is derived from the famous O I λ 7773 triplet which suffers from NLTE effects and usually pro-

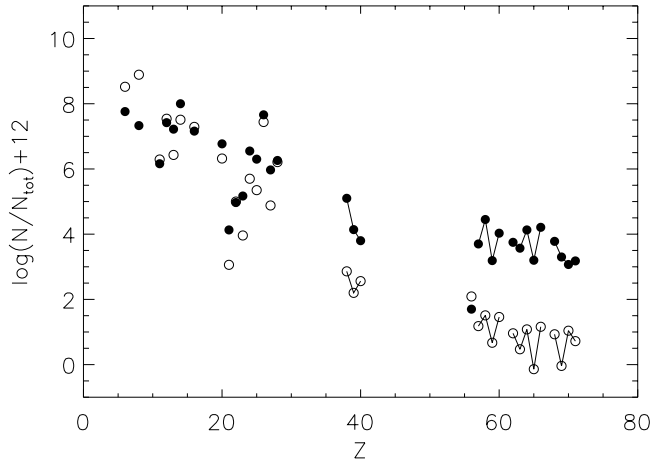


Fig. 5. Abundances for HD 166473 (filled circles) compared to the sun (open circles).

vides an incorrect overabundance when treated in LTE. Nevertheless, due to the extreme weakness of this triplet in HD 166473 we do not apply any NLTE corrections.

The sodium abundance is based on three weak, low accuracy lines. The resonance lines, however, give an order of magnitude smaller Na abundance. NLTE corrections are about -0.1 dex for main sequence stars (Mashonkina et al. 1993) and hence cannot be responsible for this large discrepancy. A model atmosphere based on ODFs also does not provide agreement between resonance and weak lines. In addition, stratification effects may play a significant role in the atmosphere, as was demonstrated for the CP star 53 Cam by Babel (1992).

A lower Mg abundance is obtained from 3 strong Mg I lines (5167, 5172, 5183 Å), but two other Mg I lines (5528 and 5711 Å) give abundances which are close to those obtained from Mg II lines. We can slightly decrease this discrepancy by applying a NLTE correction to the Mg I lines of $\leq +0.15$ dex (Mashonkina et al. 1996).

The sulphur abundance is based on four groups of S I lines centered on 6173.6, 6743.5, 6748.7, and 6757.0 Å. The first group is resolved only in the high resolution spectrum. Although all groups provide the same sulphur abundance, the last three groups show a shift of $+0.13$ Å relative to the rest of the spectrum, which is yet unexplained.

4.2. Iron peak elements

The oscillator strengths for the iron peak elements were taken from the new release of the Vienna Atomic Line Database, VALD-2, (Kupka et al. 1999, Ryabchikova et al. 1999a). The main new data sources are Lawler & Dakin (1989) for Sc II, Biémont et al. (1989) for V II, O’Brian et al. (1991), Bard et al. (1991), Bard & Kock (1994) for Fe I, and Blackwell et al. (1989), Wickliffe & Lawler (1997a) for Ni I.

We find the abundance *pattern* of the iron peak elements to be very similar to that of the other stars investigated by us so far: Ca, Ti, Fe, and Ni are the least enhanced elements and their

abundances are close to solar. Cr and Mn are more abundant, V and Co are strongly overabundant. Furthermore, the prominent overabundance of Co, determined already in all other roAp stars, is confirmed. Sc is overabundant in HD 166473 in contrast with the underabundance of this element in the other stars in our sample.

The total abundance of all iron peak elements, from Ca to Ni, results in a metallicity $[M/H] = +0.30$ which is closer to the chosen model atmosphere with $[M/H] = +0.50$ than to the value estimated previously from photometry, which was $[M/H] = +1.00$.

4.3. Sr, Y, Zr, Ba, and rare-earth elements

Sr, Y, and Zr are overabundant in HD 166473 with Y being the most anomalous element in the whole group. In contrast, Ba is deficient – as is also the case for α Cir.

The large overabundance of the rare earth elements (REE) allowed for the first time the derivation of abundances for 13 out of 14 stable REE. In the atmosphere of cool Ap stars lines of the doubly ionized REE are dominant, and therefore potentially the preferable source for an abundance determination. Unfortunately, transition probabilities have been available only since 1997. Bord et al. (1997), Wyart et al. (1997), Cowley & Bord (1997) provided calculations for the transition probabilities of Ce III, Er III, and Nd III. For Pr III we used calculations kindly provided by D. Bord (private communication). For the first ions of the REE we used oscillator strength data extracted from VALD-2. They are the same as in VALD-1 (Piskunov et al. 1995) with the exception of Dy II (Biémont & Lowe 1993), Tm II (Wickliffe & Lawler 1997b), and Lu II (Bord et al. 1998, Den Hartog et al. 1998). Abundances of all REE obtained from the lines of the first ions exceed on average the solar abundances by $+2.8$ dex. There is a marginal tendency for the lighter REE (La to Nd) being less overabundant than the heavier REE (Sm to Er).

The most striking result obtained from our REE analysis is the abundance from the second ions. They exceed the values obtained from the lines of the first ions by $+1.2$ dex (Pr), $+1.5$ dex (Nd), and $+0.7$ dex (Er), respectively. The same relative overabundance of Nd was obtained by Cowley & Bord (1998) for another roAp star, γ Equ. This observational fact cannot be explained by a wrong absolute scale of the oscillator strengths, because a similar analysis for the non-pulsating star β CrB did not indicate a significant deviation from the ionization equilibrium between the first and the second ions of the REE (Ryabchikova et al. 2000) which also means that hyperfine structure and isotopic shifts cannot be responsible for the observed differences. Pr has one stable isotope, Nd has 6 (and one with 10^{15} -yr half-life), Er has 6 stable isotopes and all three elements show similar relative overabundances of doubly ionized REE. The accuracy of the oscillator strength calculations is ± 0.15 (Cowley & Bord, 1997). The analysis of Pr and Nd lines in spectra of roAp stars definitely gives evidence for an unexpected strength of the lines of Pr III and Nd III *exclusively* relative to non-roAp stars.

Table 3. Elemental abundances for the roAp star HD 166473 ($T_{\text{eff}} = 7700$ K, $\log g = 4.20$, $[M/H] = 0.5$, $v \cdot \sin i = 0$, $v_{\text{micro}} = 0$) normalized to the total number of atoms $\log \left(\frac{N}{N_{\text{tot}}} \right)$ with formal error estimates in units of the last digit in parenthesis. Comparison with the solar abundances (Anders & Grevesse 1989), and with an abundance analysis based on an atmosphere without a magnetic field, but $v \cdot \sin i$ ranging from 15 to 40 km s⁻¹ and $v_{\text{micro}} = 1.0$ km s⁻¹ which are needed to approximate magnetic field effects. Furthermore, VALD-I was used for the latter analysis to extract the atomic parameters, but VALD-II was used for the final analysis (second column). This difference is relevant in particular for C and O, because of the new $\log gf$ values ([†]) (Wiese et al. 1996) which are now included in VALD-II. The last column lists abundances differences with and without magnetic field effects taken into account.

Species	$\log \left(\frac{N}{N_{\text{tot}}} \right)_{\text{HD}}$	lines	$\log \left(\frac{N}{N_{\text{tot}}} \right)_{\odot}$	mod. atmosphere without magn. field	lines	abundance difference
C I	-4.24(11)	8	-3.48	-3.24(51)	8	- 1.00 [†]
O I	-4.67(21)	3	-3.11	-3.92(74)	7	- 0.75 [†]
Na I	-5.84(37)	3	-5.71	-5.97(06)	2	+0.13
Mg I	-4.99(53)	5	-4.46	-4.51(38)	5	-0.48
Mg II	-4.27(31)	5	-4.46	-3.80	1	-0.47
Al I	-4.78(37)	5	-5.57	-4.89(12)	4	+0.11
Si I	-4.10(26)	10	-4.49	-3.90(35)	31	-0.20
Si II	-3.93(22)	4	-4.49	-3.59(06)	3	-0.24
S I	-4.84(10)	4	-4.71	-3.90(51)	13	-0.95
Ca I	-5.34(29)	16	-5.68	-4.87(50)	22	-0.47
Ca II	-5.12(38)	5	-5.68	-5.37	1	+0.25
Sc II	-7.87(06)	3	-8.94	-6.93(56)	4	-0.94
Ti I	-6.70	1	-7.00	-6.10(59)	4	-0.60
Ti II	-7.03(26)	5	-7.00	-6.35(41)	9	-0.67
V I	-6.60(28)	2	-8.04	-6.34(44)	3	-0.26
V II	-6.83(29)	6	-8.04			
Cr I	-5.50(45)	5	-6.30	-5.12(73)	9	-0.38
Cr II	-5.36(22)	2	-6.30	-5.07(36)	7	-0.29
Mn I	-5.70(30)	3	-6.65	-5.42(32)	7	-0.28
Mn II	-5.30	1	-6.65			
Fe I	-4.34(22)	61	-4.56	-3.80(41)	26	-0.54
Fe II	-4.31(22)	19	-4.56	-3.67(25)	14	-0.64
Co I	-6.03(12)	3	-7.12	-5.08(63)	6	-0.95
Ni I	-5.74(27)	7	-5.79	-5.28(46)	14	-0.46
Sr I	-6.90(36)	3	-9.14	-6.78(36)	2	-0.12
Sr II	-7.00	1	-9.14	-6.80	1	-0.20
Y II	-7.86(21)	7	-9.80	-7.66(58)	6	-0.20
Zr II	-8.20	2	-9.44	-7.45(42)	2	-0.75
Ba II	-10.37(06)	3	-9.91			
La II	-8.30(25)	9	-10.82	-7.11(46)	12	-1.19
Ce II	-7.55(41)	12	-10.49	-7.73(30)	6	+0.18
Pr II	-8.81(22)	15	-11.33	-8.51(20)	6	-0.30
Pr III	-7.60(38)	5				
Nd II	-7.97(28)	41	-10.54	-7.32(38)	20	-0.65
Nd III	-6.43(37)	8				
Sm II	-8.25(23)	27	-11.04	-7.46(31)	4	-0.79
Eu II	-8.43(20)	7	-11.53	-7.51(65)	8	-0.92
Gd II	-7.87(20)	9	-10.92	-7.46(35)	8	-0.41
Tb II	-8.80	2	-12.14			
Dy II	-7.79(37)	6	-10.84	-8.26(10)	3	+0.47
Er II	-8.22(17)	4	-11.07	-8.40(28)	8	+0.18
Er III	-7.50	1				
Tm II	-8.70	1	-12.04			
Yb II	-8.93(32)	3	-10.96	-8.66(36)	3	-0.27
Lu II	-8.82(27)	6	-11.28	-8.71(25)	4	-0.11

In addition, Malanushenko et al. (1998) found for γ Equ that maximum pulsation radial velocity amplitudes are observed for these 3rd spectrum REE lines.

5. Conclusions

The overall metallicity in the atmosphere of HD 166473 is larger than for all the roAp stars analyzed spectroscopically in our series (Paper I to Paper IV and the present paper). We observe a similar abundance pattern:

Rare earth elements are overabundant and C and O are less abundant than in the solar atmosphere. Ti, Fe and Ni are relatively most deficient and Co the most enhanced elements in the group of iron peak elements.

One of the most interesting features in the iron group is the clear overabundance of Co which could be detected in all five roAp stars. However, an even higher Co overabundance was determined recently by Nishimura (1998) for the hot (non-ro)A0p star HR 9049.

A new and most striking result is the discovery of the anomalous line strengths of second ions of REE resulting in an abundance increase of up to +1.5 dex, compared to abundances obtained from lines of the first ions. The latter, however, were typically used for an analysis because of a serious lack of reliable $\log gf$ values for second ions.

In agreement to Paper I to Paper IV the present study shows that roAp stars basically have similar abundances for up to 33 elements investigated in our sample, which is the most complete chemical investigation hitherto published for this group of stars. It is also the first one which discusses in detail the influence of the magnetic field on abundance analyses of CP2 stars. A comparison of rapidly oscillating to non-oscillating Ap stars does not reveal a large difference in the abundance pattern. However, one should keep in mind that the number of elements with published abundances for comparable non-roAp and “normal” stars is significantly smaller.

Oscillation periods of roAp stars are much shorter than for δ Scuti stars although they fall in the same classical instability strip. It has been speculated by Gautschy et al. (1999) that the H-He I zone at $\tau_{ross} \approx -2.5$ to 0.5 be responsible for driving roAp star pulsation. If true, the upper boundary comes close to the deepest line forming regions and hence one should expect some characteristic signatures in roAp star spectra (e.g., the observed 3rd REE spectrum anomaly?) which might allow the testing of Gautschy’s excitation model (Gautschy et al. 1998). Spectra with high signal-to-noise ratio and high spectral resolution are needed for this purpose.

For our analyses we mostly had been using Kurucz’s model atmospheres with scaled solar abundances. Strictly speaking, the abundance analysis procedure is not self consistent, because the determined abundances obviously do not follow the scaled solar abundance pattern. However, we are presently improving on this situation by calculating individual ODFs and starting to use them for computing more consistent model atmospheres. Furthermore, we intend to investigate the effects of a magnetic field on ODFs and on the structure of model atmospheres.

Acknowledgements. This research was done within the working group *Asteroseismology-AMS* supported by the Fonds zur Förderung der wissenschaftlichen Forschung (project *S 7003-AST* and *P 11882-PHY*). T.R. thanks the Russian Foundation for Basic Research for financial support (grant 98-02-16734).

References

- Anders E., Grevesse N., 1989, *Geochim. Cosmochim. Acta* 53, 197
 Babel J., 1992, *A&A* 258, 449
 Bard A., Kock M., 1994, *A&A* 282, 1014
 Bard A., Kock A., Kock M., 1991, *A&A* 248, 315
 Biémont E., Lowe R.M., 1993, *A&A* 273, 665
 Biémont E., Grevesse N., Faires L.M., et al., 1989, *A&A* 209, 391
 Blackwell D.E., Booth A.J., Petford A.D., Laming J.M., 1989, *MNRAS* 236, 235
 Bord D.J., Cowley C.R., Norquist P.L., 1997, *MNRAS* 284, 869
 Bord D.J., Cowley C.R., Mirijanian D., 1998, *Solar Phys.* 178, 221
 Cowley C.R., Bord D.J., 1997, In: Brandt J.C., Ake T.B., Petersen C.C. (eds.) *The Scientific Impact of the Goddard High Resolution Spectrograph*. ASP Conf. Ser. 143, 216
 Crawford D.L., 1979, *AJ* 84, 1858
 Den Hartog E.A., Curry J.J., Wickliffe M.E., Lawler J.E., 1998, *Solar Phys.* 178, 239
 Gautschy A., Saio H., Harzenmoser H., 1999, *MNRAS* 303, 31
 Gelbmann M., 1995, *Comm. Asteroseismology* 89
 Gelbmann M., 1998, Ph.D. Thesis, University Vienna
 Gelbmann M., Kupka F., Weiss W.W., Mathys G., 1997, *A&A* 319, 630 (Paper II)
 Hauck B., Mermilliod M., 1980, *A&AS* 40, 1
 Houk N., 1982, *Michigan Spectral Catalogue Vol. 3*, Department of Astronomy, University of Michigan, Ann Arbor
 Kupka F., Piskunov N.E., 1998, In: North P., Schnell A., Ziznovský J. (eds) *Proc. 26th Meeting and Workshop of the European Working Group on CP Stars*. *Contrib. Astron. Obs. Skalnaté Pleso* 27, 228
 Kupka F., Ryabchikova T.A., Weiss W.W., et al., 1996, *A&A* 308, 886 (Paper I)
 Kupka F., Piskunov N., Ryabchikova T.A., Stempels H.S., Weiss W.W., 1999, *A&AS* 138, 1999
 Kurtz D.W., 1982, *MNRAS* 200, 807
 Kurtz D.W., 1990, *ARA&A* 28, 607
 Kurtz D.W., Martinez P., 1987, *MNRAS* 226, 187
 Kurucz R.L., 1993, CDROM13, SAO Cambridge
 Lawer J.E., Dakin J.T., 1989, *JOSA B6*, 1457
 Malanushenko V., Savanov I., Ryabchikova T., 1998, *IBVS No.4650*, 1
 Martinez P., 1993, *The Cape Oscillating Ap Star Survey*. Ph.D. Thesis, University of Cape Town, SA
 Mashonkina L.I., Sakhbullin N.A., Shimanskij V.V., 1993, *Astron. Reports* 37, 192
 Mashonkina L.I., Shimanskaya N.N., Sakhbullin N.A., 1996, *Astron. Reports* 40, 187
 Mathys G., Hubrig S., Landstreet J.D., Lanz T., Manfroid J., 1997, *A&AS* 123, 353
 Matthews J.M., 1997, In: Provost J., Schmider F.-X. (eds.) *Sounding Solar and Stellar Interiors*. *IAU Symp.* 181, Kluwer, Dordrecht, p. 387
 Matthews J.M., Kurtz D.W., Martinez P., 1999, *ApJ* 511, 422
 Nishimura M., 1998, *PASJ* 50, 285

- O'Brian T.R., Wickliffe M.E., Lawler J.E., Whaling W., Brault J.W., 1991, JOSA B8, 1185
- Piskunov N.E., 1999, In: Nagendra K., Stenflo J. (eds.) Proc. of the 2nd International Workshop on Solar Polarization. Bangalore, India, 1998, Kluwer Acad. Publ. ASSL 243, p. 515
- Piskunov N.E., Kupka F. 2000, ApJ submitted
- Piskunov N.E., Kupka F., Ryabchikova T.A., Weiss W.W., Jeffery C.S., 1995, A&AS 112, 525
- Rogers N.Y., 1995, Comm. Asteroseismology 78
- Ryabchikova T.A., Adelman S.J., Weiss W.W., Kuschnig R., 1997a, A&A 322, 234 (Paper III)
- Ryabchikova T.A., Landstreet J.D., Gelbmann M.J., et al., 1997b, A&A 327, 1137 (Paper IV)
- Ryabchikova T., Piskunov N., Stempels H.C., Kupka F., Weiss W.W., 1999a, In: Proc. of the 6th Int. Coll. on ASOS, Victoria BC, Canada, Phys. Scripta T83, p. 162
- Ryabchikova T., Piskunov N., Savanov I., Kupka F., Malanushenko V., 1999b, A&A 343, 229
- Ryabchikova T.A., Savanov I.S., Malanushenko V.P., Kudryavtsev D.O., 2000, in preparation
- Wickliffe M.E., Lawler J.E., 1997a, ApJS 110, 163
- Wickliffe M.E., Lawler J.E., 1997b, JOSA B14, 737
- Wiese W.L., Fuhr J.R., Deters T.M., 1996, J. Phys. Chem. Ref. Data, Mono 7
- Wyart J.-F., Blaise J., Bidelman W.P., Cowley C.R., 1997, Phys. Scripta 56, 446